JGR Atmospheres

RESEARCH ARTICLE
10.1029/2019JD032269

Atmospheric Circulation as a Factor Contributing to Increasing Drought Severity in Central Europe

Ondřej Lhotka[1,2], Mirek Trnka[2], Jan Kyselý[3], Yannis Markonis[3], Jan Balek[2], and Martin Možný[2,4]

[1]Institute of Atmospheric Physics of the Czech Academy of Sciences, Prague, Czech Republic, [2]Global Change Research Institute of the Czech Academy of Sciences, Brno, Czech Republic, [3]Faculty of Environmental Sciences, Czech University of Life Sciences, Prague, Czech Republic, [4]Czech Hydrometeorological Institute, Prague, Czech Republic

Key Points:
- The 2015–2018 drought was record-breaking in the context of observational record in central Europe
- Statistically significant trends toward drier conditions were found for long-term drought indices
- Increased drought severity in the recent decades was linked to higher frequency of dry circulation types at the expense of wet types

Supporting Information:
- Supporting Information S1

Correspondence to:
O. Lhotka,
ondrej.lhotka@ufa.cas.cz

Citation:
Lhotka, O., Trnka, M., Kyselý, J., Markonis, Y., Balek, J., & Možný, M. (2020). Atmospheric circulation as a factor contributing to increasing drought severity in central Europe. *Journal of Geophysical Research: Atmospheres*, *125*, e2019JD032269. https://doi.org/10.1029/2019JD032269

Received 17 DEC 2019
Accepted 23 AUG 2020
Accepted article online 9 SEP 2020

Abstract Long-lasting and severe droughts seriously threaten agriculture, ecosystems, and society. Summer 2018 in central Europe was characterized by unusually persistent heat and drought, causing substantial economic losses, and became a part of a several years long dry period observed across this region. This study assesses the magnitude of the recent drought within a long-term context and links the increased drought severity to changes in atmospheric circulation. Temporal variability of drought conditions since the late 19th century was analyzed at seven long-term stations distributed across the Czech Republic using the Palmer Drought Severity Index and the Standardized Precipitation Evaporation Index. The Palmer *Z* Index and a variation of the Standardized Precipitation Evaporation Index were used to study rapidly emerging short-term droughts and to link these episodes to atmospheric circulation. Changes in circulation were analyzed through circulation types calculated from flow strength, direction and vorticity in mean sea level pressure data from the National Centers for Environmental Prediction (NCEP)/National Center for Atmospheric Research (NCAR) reanalysis for 1948–2018. Increasing drought severity across the Czech Republic with record-low values of the drought indices during 2015–2018 was found. The trend was distinctive in both vegetation (April–September) and cold (October–March) periods. The tendency toward more severe droughts in recent decades was linked to changes in frequency of dry and wet circulation types, highlighting the important role of atmospheric circulation in regional climate. It remains an open question whether the significantly increasing frequency of dry circulation types in the vegetation period is related to climate change, or rather represents multidecadal climate variability.

1. Introduction

Drought is a complex hazard that is dangerous through its insidious onset and large spatial extent (Spinoni et al., 2017). It is usually associated with substantial economic losses especially in agriculture (Ding et al., 2011), which are often regarded as a precursor of famine and conflicts in the rapidly growing population of the developing world (UN, 2018). Although impacts of individual drought events on global crop productivity are difficult to prove, a recent study by Trnka et al. (2019) showed a link between the size of drought-affected areas and global wheat and cereal prices. Many drought indices relying on various data and methods have been developed in order to analyze duration and severity of droughts, ranging from the relatively simple Standardized Precipitation Index (SPI; Guttman, 1998) to advanced satellite- and model-based indices (WMO & GWP, 2016). The SPI is based on the long-term precipitation record, which is fitted to a probability distribution and normalized. Its most important advantages are relatively easy calculation and feasible applicability in various climate zones. Therefore, the WMO has recommended SPI as the main meteorological drought index that countries should use to monitor drought conditions (Hayes et al., 2011).

It should be noted, however, that the absence of a temperature component in SPI limits its applicability in the warming climate, with its higher potential evapotranspiration. The compound nature of drought is better captured by indices considering changes in evapotranspiration, such as the Palmer Drought Severity Index (PDSI; Palmer, 1965) or Standardized Precipitation Evaporation Index (SPEI; Vicente-Serrano et al., 2010). Sheffield et al. (2012) showed that PDSI values depend on methods for estimating potential evapotranspiration. Use of the physically based Penman-Monteith algorithm (Allen et al., 1998) resulted in less severe drought conditions compared to the Thornthwaite (1948) approach, which is based solely on temperature.

This behavior has been especially evident since the 1980s (Sheffield et al., 2012), when a relatively rapid increase in global temperature was observed (Hartmann et al., 2013).

By contrast, Dai (2011) concluded that use of the Penman-Monteith algorithm only slightly reduces the drying trend seen in PDSI with the basic Thornthwaite model and showed increased aridity since 1950 over many land areas, especially in Africa and Southeastern Asia but also in Europe. Dai (2011) also demonstrated that the majority of this drying was due to temperature increases. In Europe, drought patterns varied over regions but a small, continuous increase of the European areas prone to drought from the early 1980s onward was found (Spinoni et al., 2015). The authors showed that Northern and Eastern Europe exhibited the largest drought frequency and severity from the 1950s to 1970s, while Western and Southern Europe (especially the Mediterranean) were struck by major droughts from the 1990s to 2010s (considering the 1950–2012 period). Increasing drought tendency in the Iberian Peninsula over recent decades was shown also by Vicente-Serrano et al. (2015), who linked this phenomenon to a greater atmospheric evaporative demand associated with temperature rise. These drier conditions over the Mediterranean are in accordance with a recent north-south polarization of drought patterns over Europe (Markonis et al., 2018).

The current study focuses on the Czech Republic, in which the shift to drier conditions is also evident. Trnka et al. (2009) found negative trends in PDSI in this region since the 1940s especially for the growing season (April–September) and linked them to the increased frequency of warm and dry "southerly", "easterly" and "high-pressure system over Central Europe" Hess-Brezowsky circulation types (Werner & Gerstengarbe, 2010). These findings are in accordance with Brázdil et al. (2015), who studied drought episodes in the 1805–2012 period using the SPEI and PDSI indices and concluded that while dry episodes in the 19th century can be attributed mainly to below-average precipitation, the most recent droughts were associated rather with the increase in temperatures. Both aforementioned studies used the Thornthwaite approach for estimating potential evapotranspiration. More detailed analyses of droughts between 1961 and 2012 showed a clear decrease of soil moisture content in the top soil layer (1 m depth), using observed and modeled time series across the Czech Republic (Trnka et al., 2015). The results are in accordance with more negative PDSI values observed in the past two decades (Brázdil et al., 2015; Trnka et al., 2009) and support suitability of the Thornthwaite method for analyzing changes in drought patterns in the Czech Republic.

Across this region, the summer of 2015 was very hot and dry (Hoy et al., 2017; Ionita et al., 2017; Lhotka, Kyselý, & Plavcová, 2018) and this drier period persisted for three more years, peaking in summer 2018, when substantial crop failures were reported along with major economic losses (EC, 2018). There are concerns whether this drying trend will continue or even accelerate due to projected increase of the global temperature (Collins et al., 2013) and more intense and longer lasting heat waves (Fischer & Schär, 2010; Lhotka, Kyselý, & Farda, 2018), during which the evaporative demand is considerably larger (Miralles et al., 2014; Stéfanon et al., 2014). The main goals of this study are to analyze severity of the central European 2015–2018 drought event in the long-term context (since the late 19th century) and study its links to atmospheric circulation. Although initial studies on severity (Skalak et al., 2019), driving mechanisms (Benedict et al., 2020), or economic impacts (Stahl et al., 2019) of the recent central European drought have been performed, we aim to analyze the 2015–2018 drought in the long-term perspective, using a robust set of data. In addition, more than 70 years of objectively classified daily pressure fields are used to link the 2015–2018 and previous droughts to atmospheric circulation. The search for drivers of drought and its trends continues to influence societal discourse in many parts of Europe, and analysis of the underlying causes is highly relevant for such debate.

2. Data and Methods

2.1. Drought Indices

The severity of droughts was assessed for seven long-term stations located in the Czech Republic, their elevations ranging roughly from 200 to 450 m above sea level (a.s.l.) (Figure 1a). The sites represent weather stations with the longest daily precipitation and temperature records available within the Czech Hydrometeorological Institute database. The study applies four drought indices (Table 1).

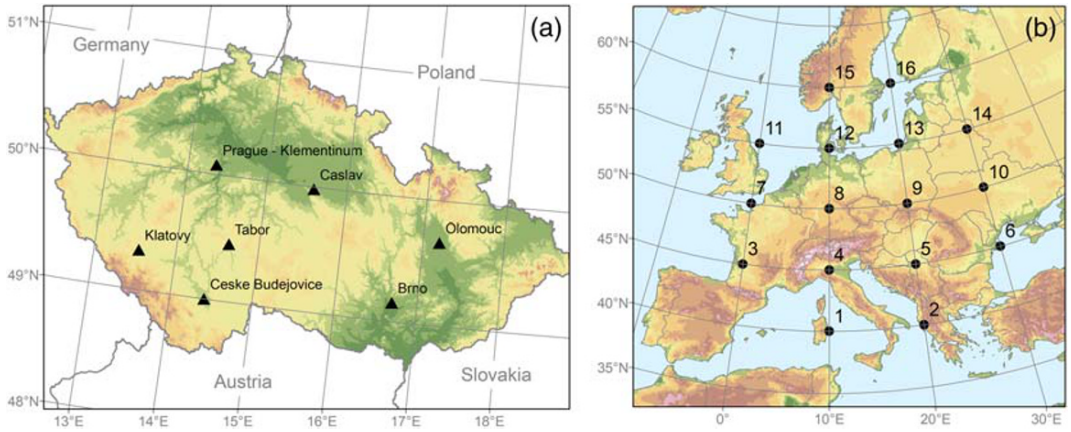

Figure 1. (a) Locations of stations used and (b) points for circulation indices' calculation.

PDSI (Palmer, 1965) was one of the first historical attempts to identify droughts using more than just precipitation data. Due to the fact that PDSI was originally calibrated with empirical constants, soil properties, and climate characteristics derived from nine stations in Kansas and Iowa (USA), its self-calibrated version (Wells et al., 2004) with a modified snow-melting module (Trnka et al., 2010) was used. In general, PDSI is based on the water supply-and-demand concept and incorporates precipitation, temperature, and water-holding capacity of soils (177.8 mm [7 in.] of precipitation was used identically for all stations). First, anomalies of water balance were calculated based on a difference between precipitation and potential evapotranspiration. Potential evapotranspiration was estimated through Thornthwaite method that is based on temperature data and latitude of a station. From the series of water balance and considering the calibration period (1912–2015), the Palmer *Z* Index (PZIN) was calculated. Finally, PDSI is then computed directly from PZIN and shows a time series of cumulative departures (with respect to previous conditions) in atmospheric moisture supply and demand – the complete algorithm is presented in Jacobi et al. (2013). Because PZIN is calculated directly from the water balance anomalies (not considering previous conditions), it responds to short-term episodes better than does PDSI and enables identifying rapidly developing drought conditions (WMO and GWP, 2016).

Another drought index applied is the SPEI (Vicente-Serrano et al., 2010). Analogously to PDSI, it is calculated based on anomalies in water balance (precipitation minus potential evapotranspiration); however, SPEI does not consider water-holding capacity of soils. Anomalies of water balance were then aggregated at 4 and 52 weeks timescales (SPEI-4 and SPEI-52) and modeled using log-logistic statistical distribution. Full documentation of SPEI is presented in Vicente-Serrano et al. (2010). In addition, a procedure that classifies precipitation as rain or snow was applied (Trnka et al., 2010). The SPEI-4 index characterizes rather short-term drought, while SPEI-52 is more suitable for analyzing long-term events.

All drought indices were calculated from temperature and precipitation data as a meteorological input, because other drought-related meteorological variables (e.g., solar radiation, wind speed, and humidity) are not available in these historical records. The indices are available in weekly temporal resolution

Table 1
Drought Indices Used

Drought index	Abbreviation	Input variables	Characteristic	Reference
Palmer Drought Severity Index	PDSI	P, T, AWC	long-term	Jacobi et al. (2013)
Palmer *Z* Index	PZIN	P, T	short-term	
Standardized Precipitation Evaporation Index (52 weeks)	SPEI-52	P, T	long-term	Vicente-Serrano et al. (2010)
Standardized Precipitation Evaporation Index (4 weeks)	SPEI-4	P, T	short-term	

Note. P = precipitation; T = temperature; AWC = available water content.

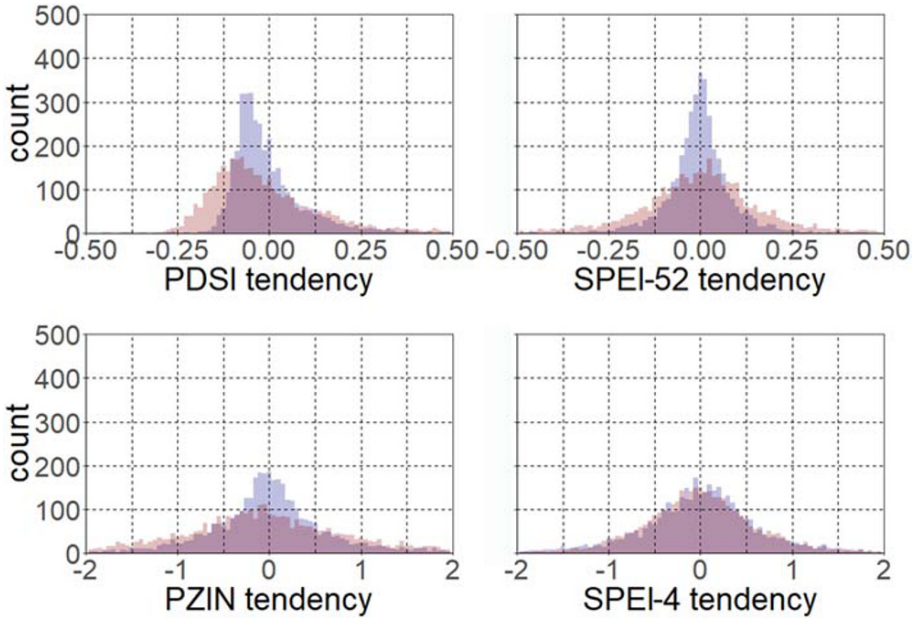

Figure 2. Distributions of weekly changes (tendencies) in the drought indices for Prague-Klementinum considering the vegetation (red) and cold (blue) periods. Drought indices' abbreviations are listed in Table 1.

(52 values per year) from the start of the individual stations' observation to 2018. The longest records are for Prague-Klementinum and Tabor (1876–2018, 143 years) while the shortest series at Klatovy starts in 1922 (97 years).

The individual drought indices respond differently to changes in input variables. Distributions of weekly changes in the drought indices (hereafter referred to as tendencies) are shown in Figure 2 (example for Prague, the results are analogous for the other stations). The tendencies were calculated separately for the vegetation period (VEG, weeks 14–39, roughly April–September) and the cold period (COLD, weeks 40–13, approximately October–March). There were significant differences between VEG and COLD in the shapes of their distributions (according to the Kolmogorov-Smirnov test at the 5% level), except for SPEI-4. The PDSI, PZIN, and SPEI-52 distributions had lower kurtosis in VEG, indicating higher frequency of extreme values compared to COLD. In addition, PDSI was positively skewed in both seasons, which suggests, for example, that positive tendencies larger than 0.25 are more abundant than negative tendencies below −0.25 (Figure 2). This is related to inclusion of the soil water-holding capacity in PDSI. The maximum soil water-holding capacity can be reached in a relatively short time during heavy rains; however, its depletion is a rather long-term process (Palmer, 1965). As expected, the short-term drought indices (PZIN and SPEI-4) exhibited larger values of weekly tendencies compared to the long-term ones, and thus, they are more suitable for linking drought to changes in atmospheric circulation.

2.2. Circulation Indices and Types

Atmospheric circulation over central Europe was characterized by circulation types derived from circulation indices. The indices (flow strength, direction, and vorticity; Jenkinson & Collison, 1977; Blenkinsop et al., 2009) were calculated at the daily timescale using sea level pressure at 16 points regularly distributed across Europe, centered at 50°N and 15°E (Figure 1b). The sea level pressure data were taken from the National Centers for Environmental Prediction (NCEP)/National Center for Atmospheric Research (NCAR) reanalysis (Kalnay et al., 1996), which is available from 1948 onward. The first circulation index is a flow strength (STR), which is a vector sum of western (w) and southern flow (s) components:

$$w = 0.5 \times (\mathrm{P4} + \mathrm{P5}) - 0.5 \times (\mathrm{P12} + \mathrm{P13})$$
$$s = 1.56 \times (\mathrm{P13} + 2 \times \mathrm{P9} + \mathrm{P5}) - 0.25 \times (\mathrm{P12} + 2 \times \mathrm{P8} + \mathrm{P4})$$
$$\mathrm{STR} = w + s$$

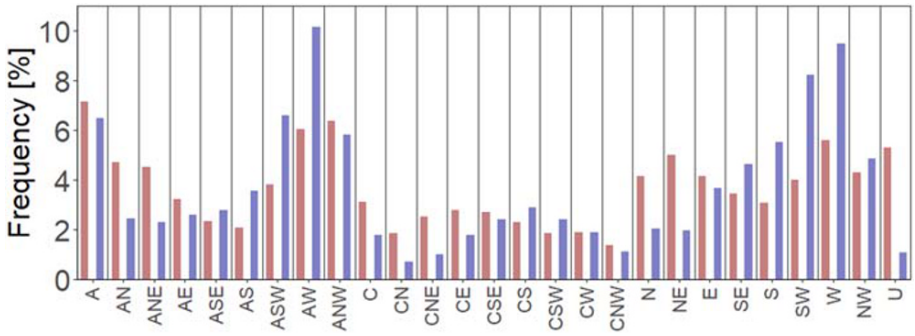

Figure 3. Frequencies of individual circulation types over central Europe for the vegetation (red) and cold (blue) periods over 1948–2018.

where P(1–16) indicate sea level pressure value for a given point in hectopascals. The second circulation index, flow direction (DIR), is calculated using a multivalued inverse tangent function and is given by the formula:

$$\mathrm{DIR} = \mathrm{atan2}(w, s)$$

The third circulation index is flow vorticity (VORT), which is the sum of its zonal (zw) and meridional (zs) components and reflects the rotation of an air mass. It indicates anticyclonic (VORT 0) or cyclonic (VORT > 0) weather conditions and is calculated using the formulas:

$$\mathrm{zw} = 1.08 \times [0.5 \times (\mathrm{P1} + \mathrm{P2}) - 0.5 \times (\mathrm{P8} + \mathrm{P9})] - 0.94 \times [0.5 \times (\mathrm{P8} + \mathrm{P9}) - 0.5 \times (\mathrm{P15} + \mathrm{P16})]$$

$$\mathrm{zs} = 1.21 \times \begin{bmatrix} 0.25 \times (\mathrm{P14} + 2 \times \mathrm{P10} + \mathrm{P6}) - 0.25 \times (\mathrm{P13} + 2 \times \mathrm{P9} + \mathrm{P5}) \\ -0.25 \times (\mathrm{P12} + 2 \times \mathrm{P8} + \mathrm{P4}) + 0.25 \times (\mathrm{P11} + 2 \times \mathrm{P7} + \mathrm{P3}) \end{bmatrix}$$

$$\mathrm{VORT} = \mathrm{zw} + \mathrm{zs}$$

In the next step, 27 circulation types based on Lamb (1972) catalogue were derived from the STR, DIR, and VORT indices. This approach was originally introduced by Jenkinson and Collison (1977) and later modified by Plavcová and Kyselý (2011) for central Europe. If STR and VORT values were lower than 4, the pressure field lacked distinctive features and that day was left unclassified (U). When the absolute value of VORT is at least five times larger than STR, strongly anticyclonic (A, if VORT 0) or strongly cyclonic (C, if VORT > 0) type was assigned. If STR was larger than the absolute value of VORT, the day was classified into one of the eight directional circulation types (N, NE, E, SE, S, SW, W, and NW). The remaining days were assigned to hybrid circulation types based on their direction and anticyclonic or cyclonic vorticity (e.g., ASW and CW). This classification was found suitable for linking atmospheric circulation to near surface temperature (Plavcová & Kyselý, 2011), precipitation (Plavcová et al., 2014), and heat waves (Lhotka, Kyselý, & Plavcová, 2018) in central Europe. Mean sea level pressure patterns related to individual circulation types are shown in Figures S1–S3 in the supporting information.

Frequencies of the circulation types in VEG and COLD are presented in Figure 3. Overall, strongly cyclonic and hybrid cyclonic circulation types were less abundant compared to their anticyclonic analogues and directional circulation types during both seasons. For VEG, the largest frequency was found for the A type (7.2%), and AW, ANW, W, and U all had frequencies larger than 5%. In COLD, by contrast, advection from the western quadrant dominates, and ASW, AW, SW, and W circulation types accounted for more than one third of days in the 1948–2018 period. The pressure field in COLD is generally more distinctive, and therefore the U circulation type appeared far less frequently in COLD compared to VEG (1.1% vs. 5.3%; Figure 3).

2.3. Linking Drought Indices to Atmospheric Circulation

Relationships between droughts and atmospheric circulation were studied through weekly tendencies of short-term drought indices (PZIN and SPEI-4), which have larger signal-to-noise ratios due to the larger

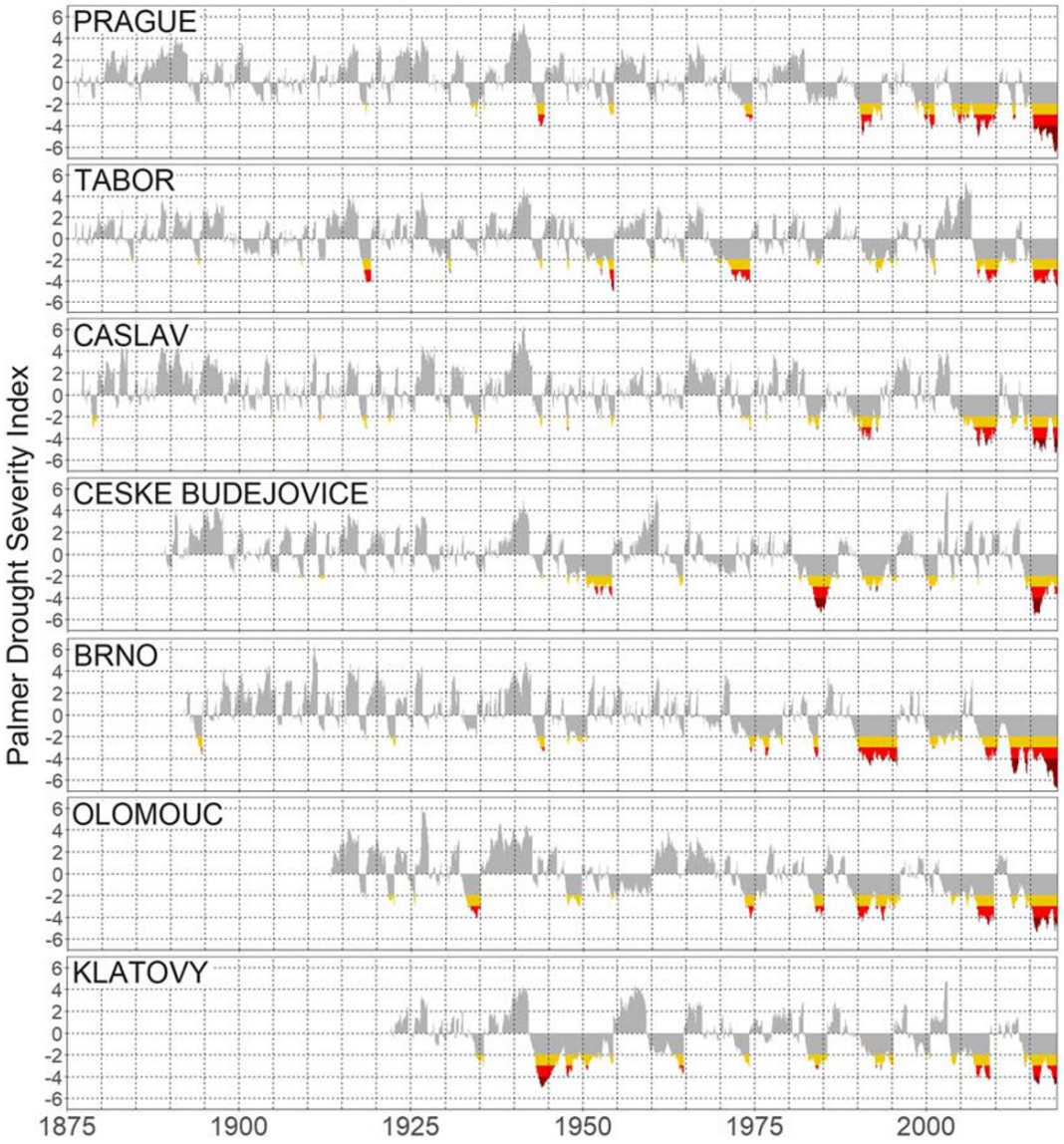

Figure 4. Temporal variability of Palmer Drought Severity Index at seven stations analyzed. Yellow color indicates moderate, red severe, and dark red extreme drought conditions.

changes between individual weeks (Figure 2). The indices were averaged across all seven stations and differences between two consecutive values were calculated. A negative tendency suggests drier conditions compared to the previous week and vice versa. Using actual drought values would not be straightforward due to a relatively long soil moisture memory (Delworth & Manabe, 1988). The drought tendencies in weekly resolution, however, cannot simply be linked to circulation types, which change on shorter timescales (Table S1). In order to overcome this issue, as many as seven daily circulation types were assigned to one weekly drought tendency value. When a single circulation type was classified during all days of the given week (which happens rather rarely), it received a weight of 7. Analogously, if two or more different circulation types occurred in the given week, they were given weights between 1 and 6 according to their duration in days within that week. For each circulation type a weighted average of tendencies was calculated for COLD and VEG in order to analyze its conduciveness to drought.

Table 2
Linear Trends of the Palmer Drought Severity Index per Decade for Seven Stations Analyzed (Sorted by Length of Available Data), Considering Four Different Time Periods

Station	Start year of data	Trend (whole period)	Trend (1922–2018)	Trend (1948–2018)	Trend (1979–2018)
Prague	1876	−0.28[a]	−0.44[a]	−0.54[a]	−0.96[a]
Tabor	1876	−0.13[a]	−0.21[a]	−0.16	−0.63[a]
Caslav	1877	−0.20[a]	−0.32[a]	−0.43[a]	−0.81[a]
Ceske Budejovice	1889	−0.18[a]	−0.17[a]	−0.08	+0.09
Brno	1892	−0.35[a]	−0.44[a]	−0.54[a]	−0.97[a]
Olomouc	1913	−0.38[a]	−0.38[a]	−0.40[a]	−0.65[a]
Klatovy	1922	−0.19[a]	−0.19[a]	−0.22[a]	−0.59[a]

[a]Denotes trends statistically significant at the 5% level.

3. Results

3.1. Temporal Variability of Drought Events

Using PDSI calculated for seven stations across the Czech Republic, long-term temporal variability of drought events was analyzed (Figure 4). The most distinctive feature recorded at all stations was the presence of extreme droughts (PDSI value lower than −4) from the 2000s onward. PDSI dropped below −6 in 2018 at stations Brno and Prague, demonstrating drought conditions unprecedented since the late 19th century (Figure 4). In Prague, extreme drought was observed from summer 2015 onward (for more than 3 years), creating the longest consecutive extreme drought event. Extreme drought episodes were recorded also prior to the 2000s, but these were not spatially coherent, for example, around 1945 (Klatovy) and 1985 (Ceske Budejovice).

All stations had negative PDSI trends (considering their whole periods of observation) ranging from −0.13 to −0.38 per decade, and similar trend values were found in the overlapping 1922–2018 period (Table 2). All trends were significant at the 5% level according to the modified Mann-Kendall trend test for autocorrelated data (Yue & Wang, 2004). Larger differences in the PDSI trends were observed during 1948–2018, a period covered by the NCEP/NCAR reanalysis that provides sea level pressure data for assessing atmospheric circulation. The most pronounced PDSI trends were found in Brno and Prague (−0.54 per decade), while the trend was close to 0 in Ceske Budejovice due to severe droughts in the 1950s and 1980s (Figure 4). The most recent 1979–2018 period (its onset corresponding with the beginning of satellite measurements) was characterized by the largest negative PDSI trends (especially in Brno, Prague, and Caslav; Table 2). Analogously to the earlier period, an indistinct statistically insignificant trend was observed in Ceske Budejovice, mainly due to the 1980s extreme drought.

In the next step, we analyzed drought episodes in more detail in VEG and COLD. The time series were averaged for all seven stations, and therefore the limited overlapping 1922–2018 period was studied. Considering PDSI, the 2015–2018 period had by far the lowest values in both seasons (with a minimum of −4.5 in VEG during 2018 and the same value was found in COLD during 2015/2016, Figure 5). This period fell outside the confidence interval defined as the $0 \pm 2 \times$ standard deviation (SD) of mean seasonal PDSI for 1922–1999. PDSI values below this interval were recorded also in 1991, 2007, and 2008 for VEG and during 1983/1984 and 2008/2009 for COLD. Confidence intervals were calculated analogously for the other drought indices.

A similar pattern was found considering another long-term index, SPEI-52. The last 4 years of observation were extremely dry especially in VEG, but the record-breaking SPEI-52 value (−2.3) was found for COLD in 2015/2016. During VEG, the record-breaking SPEI-52 (−1.8) occurred in 2007 but the 2018 season ranked as the second driest. In general, the PDSI and SPEI-52 indices showed similar temporal variability patterns for VEG and COLD, mainly due to their long-term nature—the respective seasonal values for VEG were relatively strongly correlated to those for the previous COLD season (the Pearson correlation coefficient [r] was 0.85 for PDSI and 0.74 for SPEI-52). In addition, a strong correlation between seasonal PDSI and SPEI-52 values (Figure S4) suggests a good agreement between these two indices in their ability to capture long-term drought conditions.

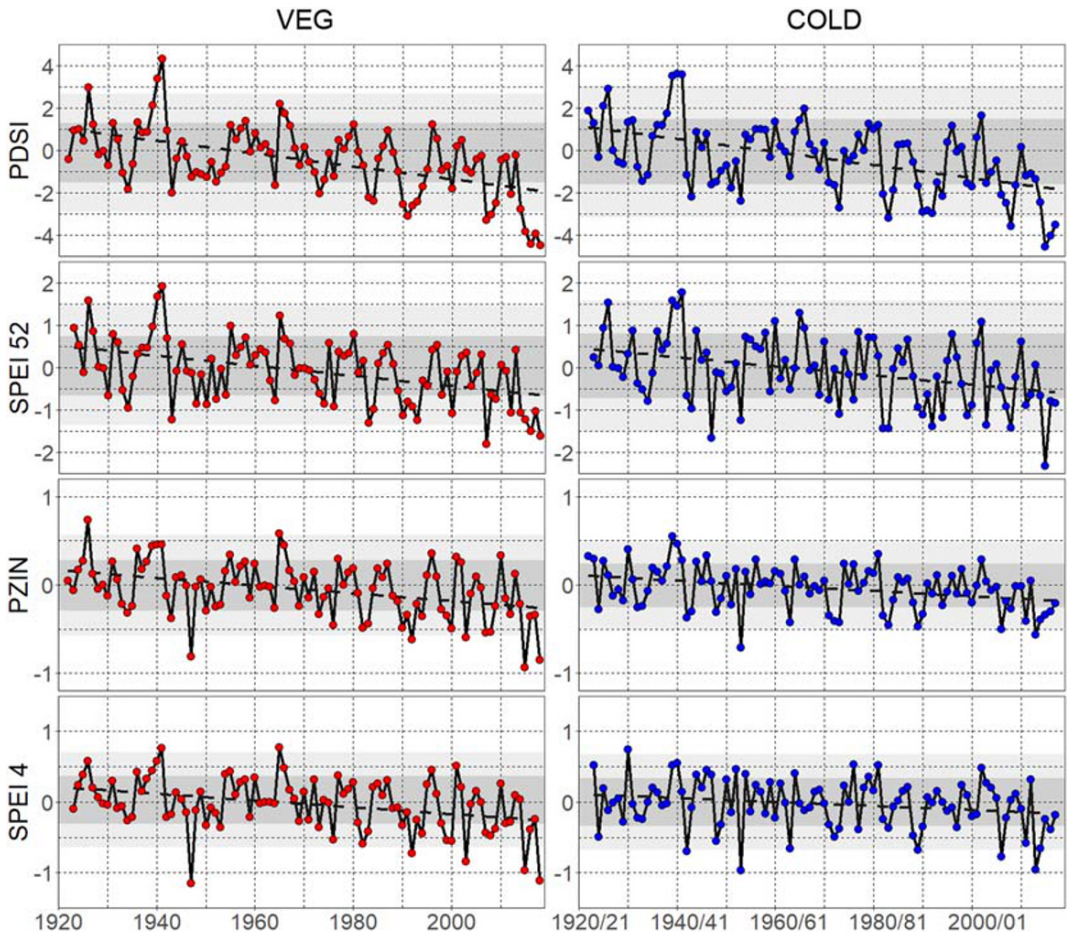

Figure 5. Temporal variability of drought indices during April–September (VEG) and October–March (COLD) seasons. The time series (1922–2018) were created by averaging drought indices from the seven stations shown in Figure 1a. Dark (light) gray zones indicate confidence intervals defined as the 0 ± 1 (2) × standard deviation of seasonal means of the respective drought index for 1922–1999.

Differences between VEG and COLD were more pronounced for short-term indices, and seasonal values of PZIN for VEG were only weakly related to those for the previous COLD season, as expected ($r = 0.37$). Moreover, seasonal SPEI-4 values for VEG were nearly independent of those for COLD ($r = 0.16$). During VEG, short-term indices revealed rapidly developing droughts in 1947, 2015, and 2018. These three seasons were linked to the three lowest values of both PZIN and SPEI-4. The driest COLD was recorded in 1953/1954, with the PZIN value of −0.7 and SPEI-4 value of −1.0. Only two other years fell outside the confidence interval in COLD as well (2006/2007 and 2013/2014), and there was good agreement between PZIN and SPEI-4, as shown in Figure S4. The long-term (PDSI and SPEI-52) indices showed significant negative trends for both seasons (using the Mann-Kendall trend test at the 5% level), which was associated with the extremely dry recent 2015–2018 period (Figure 5). Considering short-term indices, however, statistical significance was determined for PZIN in VEG only.

3.2. Links to Atmospheric Circulation

Relationships between drought indices and circulation types were analyzed for the 1948–2018 period, for which sea level pressure data from the NCEP/NCAR reanalysis were available. These circulation types were linked to drought tendencies (section 2.3) using short-term PZIN and SPEI-4 indices. Figure 6 shows mean drought tendency for each circulation type in COLD and VEG, where negative tendencies suggest increase of dry conditions and positive tendencies correspond to a wetter regime. The anticyclonic circulation types had negative mean drought tendencies (down to −0.29 considering PZIN and −0.15 for SPEI-4). By contrast, all

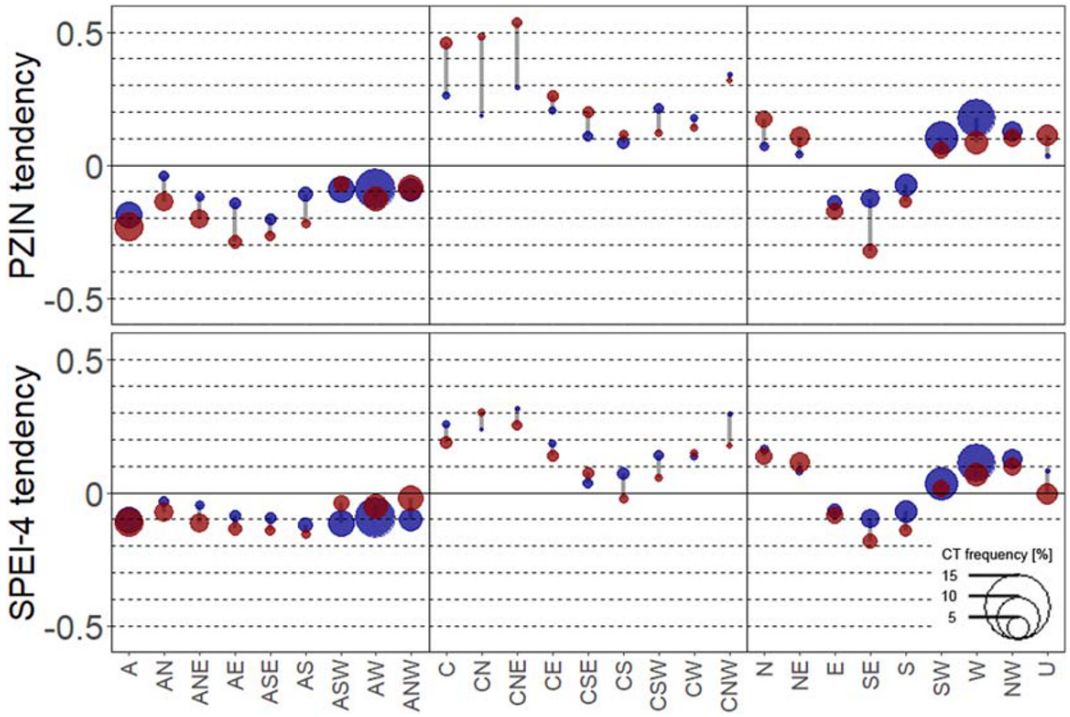

Figure 6. Mean drought tendency for 27 circulation types (CT) using two short-term drought indices, PZIN and SPEI-4. Red circles represent the vegetation period, while blue ones stand for the cold period. The size of each circle indicates the given CT frequency of occurrence. Gray guiding lines connect values of seasonal tendencies for each CT for better readability.

cyclonic circulation types were related to positive mean drought tendencies and their magnitudes were larger compared to those under anticyclonic circulation types (up to 0.55 considering PZIN and 0.31 for SPEI-4). The larger absolute values of mean drought tendencies under cyclonic circulation types were compensated by lower frequencies of these types (Figure 3). Positive drought tendencies were found also under most directional circulation types except for the easterly (E), southeasterly (SE), and southerly (S) types (Figure 6). Although a relatively large difference between mean drought tendencies in COLD and VEG appeared for some circulation types, both values always remained completely within the positive or negative sector (Figure 6). The only exception was the CS circulation type (with a low frequency of occurrence) linked to SPEI-4, which had positive mean drought tendency in COLD and slightly negative in VEG.

Based on these results, 12 circulation types with negative mean drought tendencies (averaged between PZIN and SPEI-4) were defined. Those were all anticyclonic types (A, AN, ANE, AE, ASE, AS, ASW, AW, and ANW) and directional types from the southeast quadrant (E, SE, and S; hereafter referred altogether as dry circulation types). The remaining 15 circulation types, that is, all cyclonic types (C, CN, CNE, CE, CSE, CS, CSW, CW, and CNW), directional types with northern and/or western component (NE, N, NW, W, and SW), and undefined type (U), had positive mean drought tendencies and were labeled as wet types.

The annual frequency of dry circulation types during VEG had a statistically significant (at the 1% level, according to the Mann-Kendall test) positive trend in the 1948–2018 period (roughly 2% per decade), with the largest value (68%) found in 2015. During the last 30 years, dry circulation types occurred more frequently than wet ones in 23 out of 30 VEG seasons, which is a completely opposite pattern compared to that observed in the 1950s and 1960s (Figure 7a). The droughts that fell outside the 2 × SD confidence intervals (section 3.1) occurred in those seasons in which the frequency of dry circulation types was considerably larger than the frequency of wet types. The only exception was 2007, when the number of dry and wet types was comparable. According to two-sided Student's *t* test, the mean frequency of dry circulation types during VEG

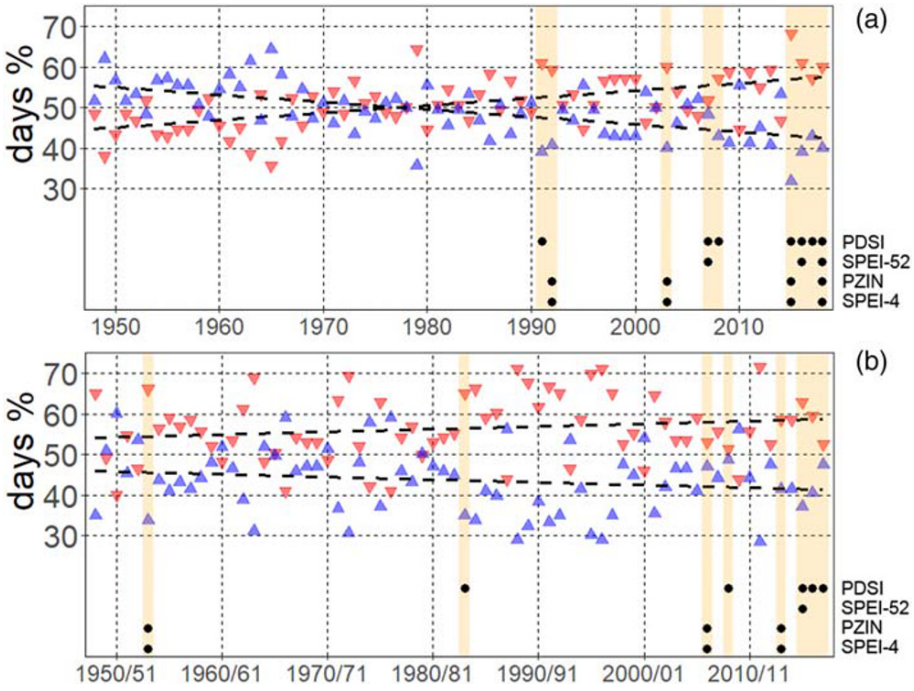

Figure 7. Temporal variability of the frequencies of dry (red) and wet (blue) circulation types with least squares regression lines, for vegetation period (a) and cold period (b). Orange polygons indicate drought periods that fell outside the 2 × SD confidence intervals (section 3.1), according to the individual drought indices (black circles).

seasons when a drought occurred was significantly (at the 1% level) larger compared to the overall mean frequency of dry types in the data set in VEG.

For COLD, the positive trend of dry circulation types' frequency had smaller magnitude (less than 1% per decade) and was not significant at the 5% level (Figure 7b). The COLD seasons in the 2015–2018 dry period had average or even below-average frequency of dry circulation types compared to other seasons and therefore the 2015–2018 drought probably originated mainly from the dryness during vegetation periods (the fact that the link between droughts and dry circulation types during COLD was weaker compared to VEG, in general, could also play a role). Although the mean frequency of dry circulation types in COLD seasons with a drought was larger than the overall mean frequency of dry types in the data set in COLD, this difference was not statistically significant.

3.3. Dry Period of 2015–2018

In this section, the dry 2015–2018 period is analyzed in more detail by linking drought indices (averaged over the stations) to individual circulation types. Prevailing wet conditions of 2013, due to floods during June in central Europe (Blöschl et al., 2013), were succeeded by a transition to a drier regime by the beginning of 2014, as reflected in the long-term indices (PDSI and SPEI-52). Only a short-term drought was observed in VEG 2013 (Figure 8), which occurred in July and August simultaneously with heat waves (Lhotka & Kyselý, 2015). The shift to drier conditions was related to unusually large number of anticyclonic and southwesterly types (A, ASW, AW, and S), at the expense of cyclonic and northerly types (Table 3), resulting in low PZIN and SPEI-4 values in the beginning of 2014 (Figure 8).

This episode was followed by moister conditions at the end of the year, partially replenishing water availability before the extreme episode of 2015. The frequency of cyclonic (anticyclonic) types was higher (lower) in VEG 2014, compared to the previous COLD 2013/2014 season (Table 3). A noteworthy lack of cyclonic types occurred in COLD 2014/15 (no C, CNE, and CNW), preceding the major drought that developed in VEG 2015. All four drought indices showed extreme drought conditions in this season and this dry period was associated with exceptionally high number of dry circulation types (especially AN, ANE, ASW, ANW, and S), while the number of cyclonic types remained low (Table 3).

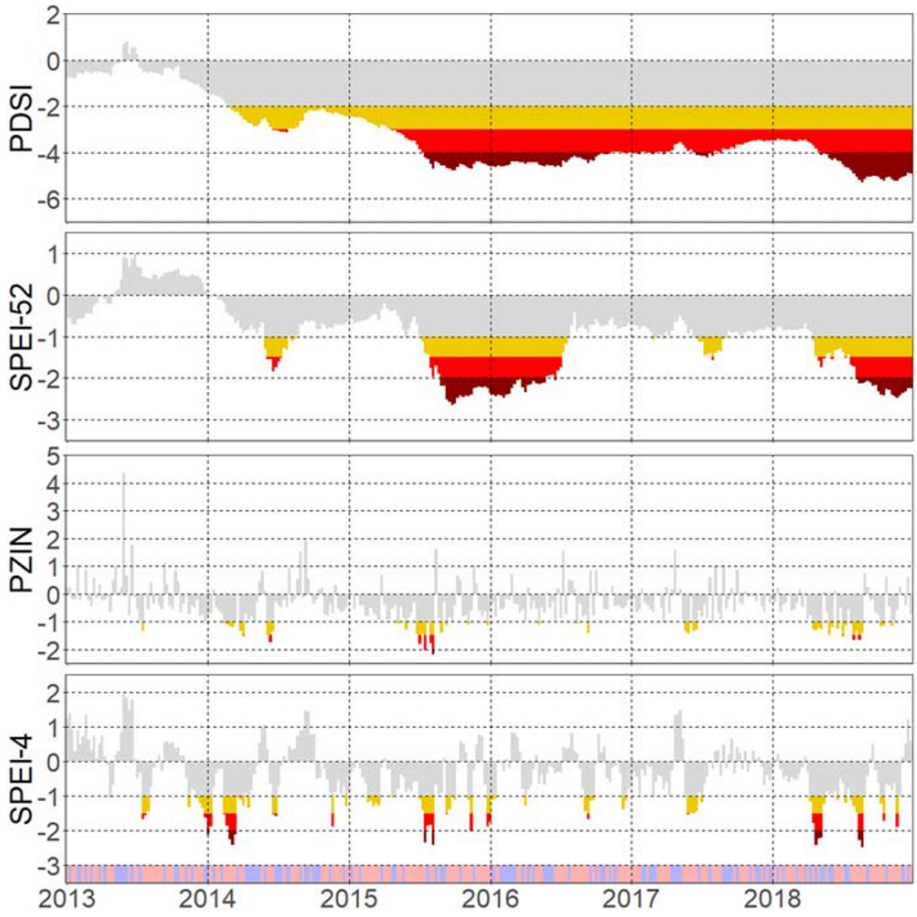

Figure 8. Temporal development of Palmer Drought Severity Index (PDSI), long-term Standardized Precipitation Evaporation Index (SPEI-52), Palmer *Z* Index (PZIN), and short-term Standardized Precipitation Evaporation Index (SPEI-4) in the 2013–2018 period. Yellow color indicates moderate, red severe, and dark red extreme drought conditions. Red (blue) bars represent weeks during which dry (wet) circulation types prevailed.

The extreme drought conditions persisted until mid-2016 (according to SPEI-52), or the end of 2016 (considering PDSI). The extreme drought was driven by unusually large abundance of dry ASW and AW types in COLD 2015/2016 and was related to the record-breaking high temperatures during this season in Europe (C3S, 2016). The largest discrepancy between the long-term drought indices was found during 2016–2017, when severe drought persisted according to PDSI, but only a short episode of moderate drought in mid-2017 was found using SPEI-52 (discussed in section 4). In 2016–2017, increased frequency of strongly anticyclonic (A) type was found in both VEG and COLD (Table 3), suggesting that advective processes were less important (compared to previous seasons) for maintaining dry conditions in this period (especially as captured by PDSI; Figure 8).

In the first half of 2018, both long-term indices dropped to severe drought level and drought conditions peaked in the second half of the year, associated with a high frequency of dry circulation types, comparable to that observed in the first half of 2015. The PDSI index reached a record-breaking value in 2018, but drought conditions were more extreme in 2015 according to SPEI-52 (Figure 8). Although the magnitude of the 2018 drought was comparable to 2015, its main driving mechanism was different. No increment in anticyclonic southerly to northwesterly types was observed (as in 2015) and the westerly advection was reduced in general (Table 3). By contrast, the frequency of dry northeasterly types (AN, ANE, AE, and E) was substantially heightened (together 52 days during VEG 2018, compared to the long-term mean of 30 days), indicating more frequent advection of dry continental air compared to previous years.

Table 3
Seasonal Numbers of Circulation Types (CT) in the 2013–2018 Period

CT	VEG2013	COLD 2013/2014	VEG 2014	COLD 2014/2015	VEG 2015	COLD 2015/2016	VEG 2016	COLD 2016/2017	VEG 2017	COLD 2017/2018	VEG 2018	VEG MEAN	COLD MEAN
A	***19**	***15**	10	12	15	9	***24**	***24**	***23**	12	***18**	13.0	11.9
AN	9	0	6	6	***12**	4	***13**	4	***13**	2	***14**	8.6	4.5
ANE	***12**	3	***13**	5	***15**	2	7	4	9	1	***14**	8.3	4.2
AE	6	2	2	2	7	5	4	***8**	0	5	***9**	5.9	4.8
ASE	4	3	3	3	*8	3	6	5	2	4	2	4.3	5.0
AS	4	8	4	7	3	7	***8**	6	5	6	3	3.8	6.5
ASW	***13**	***17**	8	***23**	***10**	***19**	***11**	12	***11**	5	6	6.9	12.1
AW	9	***25**	10	15	10	***41**	***16**	19	15	***21**	9	11.1	18.7
ANW	13	7	9	2	***22**	8	6	***15**	11	***15**	10	11.6	10.5
C	6	1	7	***0**	***1**	6	7	5	4	2	4	5.7	3.3
CN	4	2	2	1	3	2	***1**	1	4	2	2	3.4	1.3
CNE	2	***0**	6	***0**	2	1	2	4	2	2	4	4.6	1.8
CE	***1**	2	13	3	4	***0**	5	4	5	2	3	5.1	3.3
CSE	2	6	7	6	***0**	8	6	3	2	3	11	4.9	4.4
CS	8	5	2	8	2	4	***1**	8	5	4	4	4.2	5.3
CSW	4	6	3	3	3	***1**	3	4	***1**	7	3	3.4	4.4
CW	6	***1**	3	5	3	2	6	2	3	5	***0**	3.5	3.5
CNW	2	1	1	***0**	***0**	***0**	***0**	***0**	1	***0**	1	2.5	2.1
N	9	2	7	3	5	***0**	5	2	9	***1**	9	7.6	3.7
NE	8	2	13	4	***3**	4	9	3	6	3	9	9.1	3.6
E	8	6	7	5	8	6	3	3	3	***13**	***15**	7.6	6.7
SE	5	7	5	***15**	4	7	7	6	4	8	5	6.3	8.5
S	6	***14**	***8**	12	***10**	5	5	4	***8**	4	4	5.6	10.0
SW	***3**	27	7	15	11	12	***4**	14	***4**	20	8	7.3	15.0
W	7	14	8	20	10	20	***3**	13	12	24	***6**	10.2	17.4
NW	5	6	7	5	***4**	***4**	5	9	13	9	5	7.8	8.9
U	7	1	11	3	7	3	15	2	7	3	***4**	9.7	2.0

Note. Vegetation periods (VEG) and cold periods (COLD) are analyzed separately. Mean seasonal numbers calculated from the whole 1948–2018 period are shown. Highlighted numbers (bold with asterisk) indicate values larger than the seasonal mean + SD (for dry types A, AN, ANE, AE, ASE, AS, ASW, AW, ANW, E, SE, S) or lower than the seasonal mean − SD (for wet types C, CN, CNE, CE, CSE, CS, CSW, CW, CNW, N, NE, SW, W, NW, U).

4. Discussion

The analysis demonstrates that the 2015–2018 drought in the Czech Republic was of record-breaking severity on a centennial scale according to various indices. Although PDSI values indicate extreme drought condition also during the 1940s and 1980s at some stations, the spatial extent of the 2015–2018 event was unprecedented since the end of the 19th century. The extreme drought affected all stations simultaneously, revealing a characteristic homogeneity that did not occur before. These findings are also supported by empirical studies that confirm positive shifts in summer or annual evapotranspiration in central and eastern Europe (Bogawski & Bednorz, 2016; Duethman & Blöschl, 2018; Hänsel et al., 2019; Maček et al., 2018; Prăvălie et al., 2019). This shift in drought conditions is coupled with a monotonous increase in the number of days with anticyclonic conditions and/or dry advection in the vegetation period. The increased frequency of dry circulation types was observed also during the 2015–2018 drought.

Initiation of the 2015–2018 drought in central Europe coincides with the pan-European 2015 drought event (Ionita et al., 2017; Laaha et al., 2017). Although the severity of hydrological drought (streamflow levels) was not very extreme for the larger part of Europe, this was not the case for central Europe. The main reason was found in the hydrologic preconditions of each catchment (Laaha et al., 2017). According to the local hydrographs, extreme droughts occurred as a consequence of dry preconditions in the preceding winter and/or spring. In those catchments where wet preconditions prevailed, low streamflow events were less severe.

Our results are in line with this explanation. Dry conditions prevailed at all seven stations analyzed (Figure 4), and the one with the highest drought intensity in 2015 (Brno) had been experiencing the longest dry period beforehand.

It should be noted that Feng et al. (2017) reported that severity of droughts in a warmer climate might be overestimated when estimates of potential evapotranspiration are based on Thornthwaite temperature-driven approach. central Europe experienced a rapid increase of summer temperatures recently (Christidis et al., 2015) and use of the Thornthwaite method might lead to overestimation of the computed exceptional drought severity in 2015–2018. However, Feng et al. (2017) analyzed a drier and warmer region (the High Plains, USA) and the overestimation of potential evapotranspiration was found beyond the calibration period only. As the calibration period used in our study (1912–2015) includes the recent warm period, we firmly believe that the estimates of potential evapotranspiration are representative. In addition, reliable and consistent data of all input parameters needed for the Penman-Monteith formula application are rarely available especially for the period prior to 1950. Therefore, the Thornthwaite method is the only option available for estimating potential evapotranspiration in this study.

In addition, fingerprints of other significant pan-European drought events are represented in our analysis. In 1947, for instance, a well-documented drought had occurred that was followed by other drought events with lower spatial extent, marking a prolonged period of frequent droughts in Europe ending around 1954 (Moravec et al., 2019; Spinoni et al., 2015). The 1947 event is detected in the PDSI of 4 stations (Figure 4), while other consequent events are also evident at various stations, with varying initiations, durations, and terminations. The long-term fingerprint of this period (i.e., 1947–1954) can be seen in Danube streamflow, as its catchment extends over the majority of the affected regions (Pekarova et al., 2006).

The considerable difference in drought severity between PDSI and SPEI-52 from mid-2016 to mid-2018 is primarily caused by the inclusion of available soil water content into PDSI. In contrast to SPEI-52, past precipitation deficit in PDSI therefore propagates into the following weeks until soil moisture recovers to normal values (WMO and GWP, 2016). Thus, PDSI tends to capture groundwater deficits better (which was observed also during 2017; Crhová et al., 2018) while SPEI-52 seems to show more realistic drought conditions in upper soil layers during this period. In terms of drought initiation, SPEI-52 appears to better match the results of Ionita et al. (2017), who detected initiation of the 2015 event in May.

The anticyclonic and southeasterly circulation types were identified as conducive to drought. This is in accordance with Trnka et al. (2009), who used the subjective Hess-Brezowsky catalogue (Werner & Gerstengarbe, 2010) for the 1881–2005 period and found increasing abundance of dry circulation types over central Europe since the mid-20th century (considering the April–June period). The statistically significant increment in the frequency of dry advection in the vegetation period was observed also in our study, using updated data series (up to 2018) and objectively classified circulation types. This finding is also in line with Horton et al. (2015), who showed robust positive trends in the occurrence, persistence, and maximum duration of summer anticyclonic patterns over Europe in the 1979–2013 period.

A generally good agreement between increased frequency of dry circulation types and occurrence of drought was found for the vegetation period. The exceptions (e.g., in 1979 and 2007) were probably associated with simplified representation of large-scale patterns in the classification method used (e.g., absence of frontal zones; Wilby et al., 1995; no representation of processes in the atmospheric boundary layer or upper tropospheric layers; Miao et al., 2017). By contrast, a weaker link between atmospheric circulation and droughts was observed during the cold period. This phenomenon may be associated with considerably smaller potential evapotranspiration in the cold period (e.g., Burn & Hesch, 2007) and therefore lower signal-to-noise ratio compared to the vegetation period.

The increase of anticyclonic patterns in the vegetation period has a pronounced effect on drought propagation. Inasmuch as these patterns are related to both lower precipitation and higher temperatures, they accelerate soil moisture depletion. This can produce a positive feedback mechanism between soil moisture and climate (Seneviratne et al., 2006). A decline in soil moisture affects the stability of the boundary layer and reduces the frontal systems' ability to precipitate, which can exacerbate the duration and intensity of drought events. In addition, evapotranspiration is directly linked to soil moisture, which in turn impacts the flux of sensible heat and thus air temperature. A decrease in evapotranspiration means that air closer to the ground

needs a higher amount of time to cool. These feedback mechanisms are a plausible hypothesis for the link between low precipitation, increased evaporative demand, and the recent drought during the vegetation period that has been reported to be extremely severe in a 250-year time window (Hanel et al., 2018).

The persistent circulation patterns are often linked to upper-tropospheric Rossby wave-like structures (Schubert et al., 2011), which are associated with hot and dry summers over Eurasia (Röthlisberger et al., 2016). Relationships between characteristics of Rossby waves (e.g., their amplitude or propagation) and large-scale forcing have been widely discussed, with a view to rapid climate change in the Arctic (Cohen et al., 2014; Francis et al., 2017), temperature characteristics of the Atlantic Ocean (Duchez et al., 2016; Sutton & Dong, 2012), or the role of the El Nino–Southern Oscillation (Kang et al., 2014). This variety of interconnected factors makes modeling of atmospheric circulation challenging, creating relatively large uncertainties in future weather and climate extremes, including severe droughts (Woolings, 2010).

In the future climate, in general, the hydrological cycle is projected to become more intense in the warmer atmosphere, potentially resulting in increased frequency of droughts (Dai & Zhao, 2017; Prudhomme et al., 2014). On the European scale, the largest increment of drought severity is projected over the Mediterranean due to a combination of lower precipitation and higher temperatures (Spinoni et al., 2018). By contrast, modeled changes of drought severity over central Europe are inconclusive, mainly due to the simulated increase in precipitation in cold half-year (Jacob et al., 2014). The negative trends in drought indices in a warming climate of central Europe, as presented in our study, contradict these scenarios. It remains challenging for current climate models to simulate changes in atmospheric circulation, which can propagate into precipitation biases (Kotlarski et al., 2014). Other reported issues involve the lack of a robust framework for the representation of cloud microphysics (Sherwood et al., 2010), significant biases in reproducing rainfall intermittency (Trenberth et al., 2017), and the simplified representation of land-atmosphere feedbacks (Miralles et al., 2019), which may substantially intensify heat waves and droughts (Teuling, 2018).

5. Conclusions

Using four drought indices calculated at seven stations with long-term records in the Czech Republic, we studied long-term variability of droughts and their links to atmospheric circulation, with focus on the recent 2015–2018 dry period. The main findings are as follows:

1. Severity of the 2015–2018 drought was record-breaking since the late 19th century, especially when considering the long-term drought indices. PDSI values below −6 were found during this period, which was unprecedented in the observational records.
2. The dry 2015–2018 period contributed to statistically significant PDSI trends toward drier conditions over 1922–2018. Analogous results were obtained for the other long-term index, SPEI-52.
3. Short-term drought indices (PZIN and SPEI-4) showed more pronounced negative trends in the vegetation period compared to the cold period, and the dryness of 2015–2018 originated mainly from drought in the warm part of year. The two lowest PZIN values for the vegetation period were recorded in 2015 and 2018, and similar results were found for SPEI-4.
4. Frequency of dry (wet) circulation types exhibited a statistically significant positive (negative) trend for the vegetation period over 1948–2018, and this trend was in line with the observed increasing drought frequency and severity. Similar but insignificant trends in dry and wet circulation types were found also for the cold period.
5. The drought in vegetation periods during 2015–2018 was associated with above-average frequencies of dry circulation types and below-average frequencies of wet ones. The record-high seasonal abundance of dry circulation types was found in the vegetation period of 2015. Detailed analysis revealed that enhanced northeasterly advection of dry continental air contributed to advancing of the drought in 2018.

The current study highlights the strong relationship between major droughts and atmospheric circulation, implying that construction of future drought scenarios should be preceded by thorough evaluation of climate models' simulations for the recent climate, with a focus on their ability to represent observed changes in atmospheric circulation and their links to surface meteorological variables. It remains an open question, however, whether the changes in circulation patterns and the unusually large number of dry years in the

recent decades are driven by climate change or whether they are a part of natural variability of central European climate.

Data Availability Statement

Drought indices calculated for this study are available on following data repository: https://data.mendeley.com/datasets/7rfdm4bg9g/1.

Acknowledgments

O. L.'s contribution was carried within the INTER-COST project funded by the Ministry of Education, Youth and Sports of the Czech Republic (Project LTC19044). J. K. and Y. M. were supported by "XEROS: eXtremeEuRopeandrOughtS-Multimodel synthesis of past, present and future events," a bilateral project of the Czech Science Foundation (Grant 19-24089J) and the Deutsche Forschungsgemeinschaft (Grant RA 3235/1-1). M. T., J. B., and M. M. were supported by project "SustES—Adaptation strategies for sustainable ecosystem services and food security under adverse environmental conditions" (CZ.02.1.01/0.0/0.0/16_019/0000797). We acknowledge the NCEP Reanalysis data provided by the NOAA/OAR/ESRL PSD, Boulder, Colorado, USA, which can be obtained from https://www.esrl.noaa.gov/psd/data/gridded/data.ncep.reanalysis.html.

References

Allen, R. G. L., Pereira, S., Raes, D., & Smith, M. (1998). *Crop evapotranspiration: Guidelines for computing crop water requirements. FAO Report 56* (p. 300). Rome, Italy: FAO - Food and Agriculture Organization of the United Nations. Retrieved from http://www.fao.org/docrep/X0490E/X0490E00.htm

Benedict, I., van Heerwaarden, C., van der Linden, E., Weerts, A., & Hazeleger, W. (2020). Differences and similarities between the 2018 and 2003 droughts for the Rhine basin studied in terms of evaporative sources. *EGU general assembly 2020*. https://doi.org/10.5194/egusphere-egu2020-20283

Blenkinsop, S., Jones, P. D., Dorling, S. R., & Osborn, T. J. (2009). Observed and modelled influence of atmospheric circulation on central England temperature extremes. *International Journal of Climatology*, *29*(11), 1642–1660. https://doi.org/10.1002/joc.1807

Blöschl, G., Nester, T., Komma, J., Parajka, J., & Perdigao, R. A. P. (2013). The June 2013 flood in the Upper Danube Basin, and comparisons with the 2002, 1954 and 1899 floods. *Hydrology and Earth System Sciences*, *17*(12), 5197–5212. https://doi.org/10.5194/hess-17-5197-2013

Bogawski, P., & Bednorz, E. (2016). Atmospheric conditions controlling extreme summertime evapotranspiration in Poland (central Europe). *Natural Hazards*, *81*(1), 55–69. https://doi.org/10.1007/s11069-015-2066-2

Brázdil, R., Trnka, M., Mikšovský, J., Řezníčková, L., & Dobrovolný, P. (2015). Spring-summer droughts in the Czech Land in 1805–2012 and their forcings. *International Journal of Climatology*, *35*(7), 1405–1421. https://doi.org/10.1002/joc.4065

Burn, D. H., & Hesch, N. M. (2007). Trends in evaporation for the Canadian Prairies. *Journal of Hydrology*, *336*(1-2), 61–73. https://doi.org/10.1016/j.jhydrol.2006.12.011

Christidis, N., Jones, G. S., & Stott, P. A. (2015). Dramatically increasing chance of extremely hot summers since the 2003 European heatwave. *Nature Climate Change*, *5*(1), 46–50. https://doi.org/10.1038/nclimate2468

Cohen, J., Screen, J. A., Furtado, J. C., Barlov, M., Whittleston, D., Coumou, D., et al. (2014). Recent Arctic amplification and extreme mid-latitude weather. *Nature Geoscience*, *7*(9), 627–637. https://doi.org/10.1038/ngeo2234

Collins, M., Knutti, R., Arblaster, J., Dufresne, J.-L., Fichefet, T., & Friedlingstein, P. (2013). Near-term climate change: Projections and predictability. In *Climate change 2013: The physical science basis. Contribution of Working Group I to the Fifth Assessment Report of the Intergovernmental Panel on Climate Change* (pp. 953–1028). Cambridge, United Kingdom and New York, NY, USA: Cambridge University Press.

Copernicus Climate Change Service (C3S) (2016). *Average surface air temperatures for December 2015*. United Kingdom: ECMWF. Retrieved from https://climate.copernicus.eu/average-surface-air-temperatures-december-2015

Crhová, L., Čekal, R., & Černá, L. (2018). *Roční zpráva o hydrometeorologické situaci v České republice 2017 [in Czech]*. Prague, Czech Republic: Czech Hydrometeorological Institute. Retrieved from http://portal.chmi.cz/files/portal/docs/hydro/sucho/Zpravy/ROK_2017.pdf

Dai, A. (2011). Characteristics and trends in various forms of the Palmer Drought Severity Index during 1900–2008. *Journal of Geophysical Research*, *116*, D12115. https://doi.org/10.1029/2010JD015541

Dai, A., & Zhao, T. (2017). Uncertainties in historical changes and future projections of drought. Part I: Estimates of historical drought changes. *Climatic Change*, *144*(3), 519–533. https://doi.org/10.1007/s10584-016-1705-2

Delworth, T. L., & Manabe, S. (1988). The influence of potential evaporation on the variabilities of simulated soil wetness and climate. *Journal of Climate*, *1*(5), 523–547. https://doi.org/10.1175/1520-0442(1988)0010523:TIOPEO>2.0.CO;2

Ding, Y, Hayes, M. J., & Widhalm, M. (2011). Measuring economic impacts of drought: a review and discussion. *Disaster Prevention and Management: An International Journal*, *20*(4), 434–446. https://doi.org/10.1108/09653561111161752

Duchez, A., Frajka-Williams, E., Josey, S. A., Evans, D. G., Grist, J. P., Marsh, R., et al. (2016). Drivers of exceptionally cold North Atlantic Ocean temperatures and their link to the 2015 European heat wave. *Environmental Research Letters*, *11*(7), 074004. https://doi.org/10.1088/1748-9326/11/7/074004

European Commision (EC) (2018). *Report: EU agricultural markets short-term outlook-Autumn 2018*. Brussels, Belgium: European Commision. Retrieved from https://ec.europa.eu/info/sites/info/files/food-farming-fisheries/farming/documents/agri-short-term-outlook-reports_2018.zip

Feng, S., Trnka, M., Hayes, M., & Zhang, Y. (2017). Why do different drought indices show distinct future drought risk outcomes in the U.S. Great Plains? *Journal of Climate*, *30*(1), 265–278. https://doi.org/10.1175/JCLI-D-15-0590.1

Fischer, E. M., & Schär, C. (2010). Consistent geographical patterns of changes in high-impact European heatwaves. *Nature Geoscience*, *3*(6), 398–403. https://doi.org/10.1038/ngeo866

Francis, J. A., Vavrus, S. J., & Cohen, J. (2017). Amplified Arctic warming and mid-latitude weather: New perspectives on emerging connections. *Wiley Interdisciplinary Reviews: Climate Change*, *8*(5), 1–11. https://doi.org/10.1002/wcc.474

Guttman, N. B. (1998). Comparing the Palmer drought index and the standardized precipitation index. *Journal of the American Water Resources Association*, *34*(1), 113–121. https://doi.org/10.1111/j.1752-1688.1998.tb05964

Hanel, M., Rakovec, O., Markonis, Y., Máca, P., Samaniego, L., Kyselý, J., & Kumar, R. (2018). Revisiting the recent European droughts from a long-term perspective. *Scientific Reports*, *8*(1), 9499. https://doi.org/10.1038/s41598-018-27464-4

Hänsel, S., Ustrnul, Z., Lupikasza, E., & Skalak, P. (2019). Assessing seasonal drought variations and trends over Central Europe. *Advances in Water Resources*, *127*, 53–75. https://doi.org/10.1016/j.advwatres.2019.03.005

Hayes, M., Svoboda, M., Wall, N., & Widhalm, M. (2011). The Lincoln declaration on drought indices: Universal meteorological drought index recommended. *Bulletin of the American Meteorological Society*, *92*(4), 485–488. https://doi.org/10.1175/2010bams3103.1

Horton, D. E., Johnson, N. C., Singh, D., Swain, D. L., Rajaratnam, B., & Diffenbaugh, N. S. (2015). Contribution of changes in atmospheric circulation patterns to extreme temperature trends. *Nature*, *522*(7557), 465–469. https://doi.org/10.1038/nature14550

Hoy, A., Hänsel, S., Skalak, P., Ustrnul, Z., & Bochníček, O. (2017). The extreme European summer of 2015 in a long-term perspective. *International Journal of Climatology*, *37*(2), 943–962. https://doi.org/10.1002/joc.4751

Ionita, M., Tallaksen, L. M., Kingston, D. G., Stagge, J. H., Laaha, G., & Van Lanen, H. A. J. (2017). The European 2015 drought from a climatological perspective. *Hydrology and Earth System Sciences*, *21*(3), 1397–1419. https://doi.org/10.5194/hess-21-1397-2017, https://doi.org/10.5194/hess-21-1397-2017

Jacob, D., Petersen, J., Eggert, B., Alias, A., Christensen, O. B., Bouwer, L. M., et al. (2014). EURO-CORDEX: New high-resolution climate change projections for European impact research. *Regional Environmental Change*, *14*(2), 563–578. https://doi.org/10.1007/s10113-013-0499-2

Jacobi, J., Perrone, D., Duncan, L. L., & Hornberger, G. (2013). A tool for calculating the Palmer drought indices. *Water Resources Research*, *49*, 6086–6089. https://doi.org/10.1002/wrcr.20342

Jenkinson, A. F., & Collison, F. P. (1977). An initial climatology of gales over the North Sea. In *Synoptic climatology branch memorandum no. 62*. Bracknell, United Kingdom: Meteorological Office.

Kalnay, E., Kanamitsu, M., Kistler, R., Collins, W., Deaven, D., Gandin, L., et al. (1996). The NCEP/NCAR 40-year reanalysis project. *Bulletin of the American Meteorological Society*, *77*(3), 437–471. https://doi.org/10.1175/1520-0477(1996)0770437:TNYRP>2.0.CO;2

Kang, I.-S., No, H.-H., & Kucharski, F. (2014). ENSO amplitude modulation associated with the mean SST changes in the tropical Central Pacific induced by Atlantic multidecadal oscillation. *Journal of Climate*, *27*(20), 7911–7920. https://doi.org/10.1175/JCLI-D-14-00018.1

Hartmann, D. L., Klein Tank, A. M. G., Rusticucci, M., Alexander, L. V., Brönnimanm, S., & Charabi, J. A.-R. (2013). Observations: Atmosphere and Surface. In *Climate change 2013, The physical science basis. Contribution of Working Group I to the Fifth Assessment Report of the Intergovernmental Panel on Climate Change* (pp. 159–254). Cambridge, United Kingdom and New York, NY, USA: Cambridge University Press.

Kotlarski, S., Keuler, K., Christensen, O. B., Collete, A., Déqué, M., Gobiet, A., et al. (2014). Regional climate modeling on European scales: A joint standard evaluation of the EURO-CORDEX RCM ensemble. *Geoscientific Model Development*, *7*(4), 1297–1333. https://doi.org/10.5194/gmd-7-1297-2014

Laaha, G., Gauster, T., Tallaksen, L. M., Vidal, J. P., Stahl, K., Prudhomme, C., et al. (2017). The European 2015 drought from a hydrological perspective. *Hydrology and Earth System Sciences*, *21*(6), 3001–3024. https://doi.org/10.5194/hess-21-3001-2017

Lamb, H. H. (1972). British Isles Weather types and a register of daily sequence of circulation patterns, 1861–1971. In *Geophysical Memoir 116* (pp. 1–85). London: HMSO.

Lhotka, O., & Kyselý, J. (2015). Hot central-European summer of 2013 in a long-term context. *International Journal of Climatology*, *35*(14), 4399–4407. https://doi.org/10.1002/joc.4277

Lhotka, O., Kyselý, J., & Farda, A. (2018). Climate change scenarios of heat waves in Central Europe and their uncertainties. *Theoretical and Applied Climatology*, *131*(3-4), 1043–1054. https://doi.org/10.1007/s00704-016-2031-3

Lhotka, O., Kyselý, J., & Plavcová, E. (2018). Evaluation of major heat waves' mechanisms in EURO-CORDEX RCMs over Central Europe. *Climate Dynamics*, *50*(11-12), 4249–4262. https://doi.org/10.1007/s00382-017-3873-9

Maček, U., Bezak, N., & Šraj, M. (2018). Reference evapotranspiration changes in Slovenia, Europe. *Agricultural and Forest Meteorology*, *260-261*, 183–192. https://doi.org/10.1016/j.agrformet.2018.06.014

Markonis, Y., Hanel, M., Máca, P., Kyselý, J., & Cook, E. R. (2018). Persistent multi-scale fluctuations shift European hydroclimate to its millennial boundaries. *Nature Communications*, *9*(1), 1767–1712. https://doi.org/10.1038/s41467-018-04207-7

Miao, Y., Guo, J., Liu, S., Liu, H., Li, Z., Zhang, W., & Zhai, P. (2017). Classification of summertime synoptic patterns in Beijing and their associations with boundary layer structure affecting aerosol pollution. *Atmospheric Chemistry and Physics*, *17*(4), 3097–3110. https://doi.org/10.5194/acp-17-3097-2017

Miralles, D. G., Gentine, P., Seneviratne, S. I., & Teuling, A. J. (2019). Land-atmospheric feedbacks during droughts and heatwaves: State of the science and current challenges. *Annals of the New York Academy of Sciences*, *1436*(1), 19–35. https://doi.org/10.1111/nyas.13912

Miralles, D. G., Teuling, A. J., Van Heerwaarden, C. C., & Vilà-Guerau de Arellano, J. (2014). Mega-heatwave temperatures due to combined soil desiccation and atmospheric heat accumulation. *Nature Geoscience*, *7*(5), 345–349. https://doi.org/10.1038/ngeo2141

Moravec, V., Markonis, Y., Rakovec, O., Kumar, R., & Hanel, M. (2019). A 250-year European drought inventory derived from ensemble hydrologic modelling. *Geophysical Research Letters*, *46*, 5909–5917. https://doi.org/10.1029/2019GL082783

Palmer, W. C. (1965). *Meteorological drought. Research paper No. 45*. Washington, DC: US weather bureau.

Pekarova, P., Miklanek, P., & Pekar, J. (2006). Long-term trends and runoff fluctuations of European rivers. *Climate Variability and Change—Hydrological Impacts* (pp. 520–525). Wallingford, United Kingdom: IAHS Press. Retrieved from https://iahs.info/uploads/dms/13714.94-520-525-97-308-Pekarova.pdf

Plavcová, E., & Kyselý, J. (2011). Evaluation of daily temperatures in Central Europe and their links to large-scale circulation in an ensemble of regional climate models. *Tellus A*, *63A*, 763–781. https://doi.org/10.1111/j.1600-0870.2011.00514.x

Plavcová, E., Kyselý, J., & Štěpánek, P. (2014). Links between circulation types and precipitation in Central Europe in the observed data and regional climate model simulations. *International Journal of Climatology*, *34*(9), 2885–2898. https://doi.org/10.1002/joc.3882

Prăvălie, R., Piticar, A., Roşca, B., Sfică, L., Bandoc, G., Tiscovschi, A., & Patriche, C. (2019). Spatio-temporal changes of the climatic water balance in Romania as a response to precipitation and reference evapotranspiration trends during 1961–2013. *Catena*, *172*, 295–312. https://doi.org/10.1016/j.catena.2018.08.028

Prudhomme, C., Giuntoli, I., Robinson, E. L., Clark, D. B., Arnell, N. W., Dankers, R., et al. (2014). Hydrological droughts in the 21st century, hotspots and uncertainties from a global multimodel ensemble experiment. *Proceedings of the National Academy of Sciences*, *111*, 3262–3267.

Röthlisberger, M., Pfahl, S., & Martius, O. (2016). Regional-scale jet waviness modulates the occurrence of midlatitude weather extremes. *Geophysical Research Letters*, *43*, 10,989–10,997. https://doi.org/10.1002/2016GL070944

Schubert, S., Wang, H., & Suarez, M. (2011). Warm season subseasonal variability and climate extremes in the northern hemisphere: The role of stationary Rossby waves. *Journal of Climate*, *24*(18), 4773–4792. https://doi.org/10.1175/JCLI-D-10-05035.1

Seneviratne, S. I., Lüthi, D., Litschi, D., & Schär, C. (2006). Land–atmosphere coupling and climate change in Europe. *Nature*, *443*(7108), 205–209. https://doi.org/10.1038/nature05095

Sheffield, J., Wood, E. F., & Roderick, M. L. (2012). Little change in global drought over the past 60 years. *Nature*, *491*(7424), 435–438. https://doi.org/10.1038/nature11575

Sherwood, S. C., Roca, R., Weckwerth, T. M., & Andronova, N. G. (2010). Tropospheric water vapor, convection, and climate. *Reviews of Geophysics*, *48*, RG2001. https://doi.org/10.1029/2009RG000301

Skalak, P., Stepanek, P., Zahradnicek, P., & Trnka, M. (2019). Extreme drought of 2018 in the Czech Republic. *Geophysical Research Abstracts*, *21*, EGU2019–EGU11262. https://meetingorganizer.copernicus.org/EGU2019/EGU2019-11262.pdf

Spinoni, J., Naumann, G., & Vogt, J. V. (2017). Pan-European seasonal trends and recent changes of drought frequency and severity. *Global and Planetary Change*, *148*, 113–130. https://doi.org/10.1016/j.gloplacha.2016.11.013

Spinoni, J., Naumann, G., Vogt, J. V., & Barbosa, P. (2015). The biggest drought events in Europe from 1950 to 2012. *Journal of Hydrology: Regional Studies*, *3*, 509–524. https://doi.org/10.1016/j.ejrh.2015.01.001

Spinoni, J., Vogt, J. V., Naumann, G., Barbosa, P., & Dosio, A. (2018). Will drought events become more frequent and severe in Europe? *International Journal of Climatology*, *38*(4), 1718–1736. https://doi.org/10.1002/joc.5291

Stahl, K., Blauhut, V., Stoelzle, M., Tijdeman, E., Menzel, L., & Lange, J. (2019). Linking multi-sectorial impacts to hydrometeorological extremes duringthe drought of 2018 in Germany. *Geophysical Research Abstracts*, *21*, EGU2019–EGU10549.

Stéfanon, M., Drobinski, P., D'Andrea, F., & Brossier, C. L. (2014). Soil moisture-temperature feedbacks at meso-scale during summer heat waves over Western Europe. *Climate Dynamics*, *42*(5-6), 1309–1324. https://doi.org/10.1007/s00382-013-1794-9

Sutton, R. T., & Dong, B. (2012). Atlantic Ocean influence on a shift in European climate in the 1990s. *Nature Geoscience*, *5*(11), 788–792. https://doi.org/10.1038/ngeo1595

Teuling, A. J. (2018). A hot future for European droughts. *Nature Climate Change*, *8*(5), 364–365. https://doi.org/10.1038/s41558-018-0154-5

Thornthwaite, C. W. (1948). Anapproach toward a rational classification of climate. *Geographical Review*, *38*(1), 55–94. https://doi.org/10.2307/210739

Trenberth, K. E., Zhang, Y., & Gehne, M. (2017). Intermittency in precipitation: Duration, frequency, intensity, and amounts using hourly data. *Journal of Hydrometeorology*, *18*(5), 1393–1412. https://doi.org/10.1175/JHM-D-16-0263.1

Trnka, M., Brázdil, R., Možný, M., Štěpánek, P., Dobrovolný, P., Zahradníček, P., et al. (2015). Soil moisture trends in the Czech Republic between 1961 and 2012. *International Journal of Climatology*, *35*(13), 3733–3747. https://doi.org/10.1002/joc.4242

Trnka, M., Feng, S., Semenov, M. A., Olesen, J. E., Kersebaum, K. C., Rötter, R. P., et al. (2019). Mitigation efforts will not fully alleviate the increase in water scarcity occurrence probability in wheat-producing areas. *Science Advances*, *5*. https://doi.org/10.1126/sciadv.aau2406

Trnka, M., Kocmánková, E., Balek, J., Eitzinger, J., Ruget, F., Formayer, H., et al. (2010). Simple snow cover model for agrometeorological applications. *Agricultural and Forest Meteorology*, *150*(7-8), 1115–1127. https://doi.org/10.1016/j.agrformet.2010.04.012

Trnka, M., Kyselý, J., Možný, M., & Dubrovský, M. (2009). Changes in central-European soil-moisture availability and circulation patterns in 1881–2005. *International Journal of Climatology*, *29*(5), 655–672. https://doi.org/10.1002/joc.1703

United Nations (UN) (2018). *Drought and conflict leave millions more hungry in 2017–UN–backed report*. Rome, Italy: UN World Food Programme (WFP) and Food and Agriculture Organization (FAO). Retrieved from https://news.un.org/en/story/2018/03/1005621

Vicente-Serrano, S. M., Begueria, S., & Lopez-Moreno, J. I. (2010). A multi-scalar drought index sensitive to global warming: The standardized precipitation evapotranspiration index. *Journal of Climate*, *23*(7), 1696–1718. https://doi.org/10.1175/2009JCLI2909.1

Vicente-Serrano, S. M., Lopez-Moreno, J.-I., Beguería, S., Lorenzo-Lacruz, J., Sanchez-Lorenzo, A., García-Ruiz, J. M., et al. (2015). Evidence of increasing drought severity caused by temperature rise in southern Europe. *Environmental Research Letters*, *9*(4), 044001. https://doi.org/10.1088/1748-9326/9/4/044001

Wells, N., Goddard, S., & Hayes, M. J. (2004). A self-calibrating Palmer drought severity index. *Journal of Climate*, *17*(12), 2335–2351. https://doi.org/10.1175/1520-0442(2004)0172335:ASPDSI>2.0.CO;2

Werner, P. C., & Gerstengarbe, F. V. (2010). *Katalog der grosswetterlagen Europas (1881–2009)*, *PIK Report* (Vol. 119). Potsdam: Potsdam Institute for Climate Impact Research.

Wilby, R. L., Barnsley, N., & O'Hare, G. (1995). Rainfall variability associated with Lamb weather types: The case for incorporating weather fronts. *International Journal of Climatology*, *15*(11), 1241–1252. https://doi.org/10.1002/joc.3370151105

Woolings, T. (2010). Dynamical influences on European climate: An uncertain future. *Philosophical Transactions of the Royal Society A: Mathematical, Physical and Engineering Sciences*, *368*(1924), 3733–3756. https://doi.org/10.1098/rsta.2010.0040

World Meteorological Organization (WMO) and Global Water Partnership (GWP) (2016). *Handbook of drought indicators and indices*. Geneva: World Meteorological Organization and Global Water Partnership. ISBN: 978-92-63-11173-9. https://www.droughtmanagement.info/literature/GWP_Handbook_of_Drought_Indicators_and_Indices_2016.pdf

Yue, S., & Wang, C. Y. (2004). The Mann-Kendall test modified by effective sample size to detect trend in serially correlated hydrological series. *Water Resources Management*, *18*(3), 201–218. https://doi.org/10.1023/B:WARM.0000043140.61082.60